Updated 6–11-Month Prediction of Atlantic Basin Seasonal Hurricane Activity

PHILIP J. KLOTZBACH AND WILLIAM M. GRAY

Department of Atmospheric Science, Colorado State University, Fort Collins, Colorado

(Manuscript received 9 December 2003, in final form 23 April 2004)

ABSTRACT

An updated statistical scheme for forecasting seasonal tropical cyclone activity in the Atlantic basin by 1 December of the previous year is presented. Previous research by Gray and colleagues at Colorado State University showed that a statistical forecast issued on 1 December of the previous year could explain up to about 50% of the jackknife hindcast variance for the 1950–90 time period. Predictors utilized in the original forecast scheme included a forward extrapolation of the quasi-biennial oscillation (QBO) and two measures of West African rainfall. This forecast has been issued since 1991 but has shown little skill because of the as yet unexplained failure of the West African rainfall predictors during the 1990s.

The updated scheme presented in this paper does not utilize West African rainfall predictors. It employs the new NCEP–NCAR reanalysis data and involves predictors that span the globe. Much experimentation has led to the choosing of conditions associated with the El Niño-Southern Oscillation (ENSO), the Arctic Oscillation (AO), the North Atlantic Oscillation (NAO), the Pacific–North American pattern (PNA), and the QBO. This new statistical scheme shows similar cross-validated (jackknifed) hindcast skill to the original scheme (explaining up to about 50% of the variance) but is developed over a decade longer time period (1950–2001). In addition, since all predictors are taken directly from the NCEP–NCAR reanalysis, one does not need to consider rainfall collection issues that have caused major problems with the West African rainfall data since 1995. Hypothetical physical linkages between the predictors and the following year's hurricane activity are also presented. Based on the net tropical cyclone (NTC) activity prediction and a weighted average of North Atlantic sea surface temperatures, forecasts of U.S. hurricane landfall probability that showed considerable hindcast skill over the 52-yr period of 1950–2001 can also be issued.

1. Introduction

The Atlantic basin (the Atlantic Ocean north of the equator, the Caribbean Sea, and the Gulf of Mexico) has more year-to-year variability in tropical cyclone (TC) activity than any other hurricane region. For example, there were 12 hurricanes in 1969 and 11 hurricanes in 1995, but only 2 hurricanes formed in 1982. Intense hurricanes (category 3–4–5 on the Saffir–Simpson scale) also vary considerably from year to year. Seven intense hurricanes developed in 1950, whereas no intense hurricanes formed in 1962, 1968, 1972, 1986, and 1994. These examples illustrate the considerable differences in Atlantic hurricane activity that occur on a year-to-year basis.

Gray (1984a,b) was the first to propose that large-scale features could be used to predict Atlantic basin seasonal hurricane activity. The original predictors involved the state of two global modes: El Niño–Southern Oscillation (ENSO) and the quasi-biennial oscillation (QBO). In addition, regional Caribbean Basin sea level pressure anomalies were included in the original scheme. Cool ENSO conditions, west-phase QBO conditions, and low sea level pressures in the Caribbean Basin were all associated with increased Atlantic basin tropical cyclone activity. Forecasts for the current year's hurricane season were issued in early June and early August between 1984 and 1991.

Extended-range seasonal forecasts were issued beginning in 1992 with the development of a long-range statistical forecast of Atlantic basin seasonal hurricane activity. Gray et al. (1992a) found that cross-validated hindcast skill explaining approximately 50% of the variance in Atlantic basin tropical cyclone activity could be obtained based on the 1950–90 time period. This first-ever 1 December forecast utilized predictors involving West African rainfall and the QBO. They extrapolated the QBO 10 months into the future to estimate the wind strength at 30 mb, 50 mb, and the shear between these levels for the following September. Rainfall in the western Sahel during August–September of the previous year and rainfall in the Gulf of Guinea during August–November of the previous year was utilized as African rainfall predictors.

Years that were in the west phase of the QBO were found to have many more intense hurricanes. Gray et

Corresponding author address: Philip J. Klotzbach, Department of Atmospheric Science, Colorado State University, Fort Collins, CO 80523.
E-mail: philk@atmos.colostate.edu

TABLE 1. Early-Dec forecast and observed values of hurricane days and hurricane destruction potential for 1992–2002. The average difference between forecast and observed values was taken without respect to sign.

Year	Forecast hurricane days	Observed hurricane days	Difference	Forecast hurricane destruction potential	Observed hurricane destruction potential	Difference
1992	15	16	−1	35	51	−16
1993	25	10	15	75	23	52
1994	25	7	18	85	15	70
1995	35	62	−27	100	173	−73
1996	20	45	−25	50	135	−85
1997	25	10	15	75	26	49
1998	20	49	−29	50	145	−95
1999	40	43	−3	130	145	−15
2000	25	32	−7	85	85	0
2001	20	27	−7	65	71	−6
2002	35	11	24	90	31	59
Average difference			|15.5|			|47.3|
R^2			0.07			0.03
Jackknife hindcast R^2 (1950–90)			0.51			0.53

al. (1992a) hypothesized that lower-stratospheric wind ventilation was reduced during west-phase years. In addition, the west phase of the QBO has been shown to enhance off-equatorial convection, while equatorial convection is favored in east QBO years (Gray et al. 1992b; Knaff 1993). Since hurricanes do not form within 5° of the equator, off-equatorial convection is more favorable for African easterly waves developing into tropical cyclones. The West African rainfall–tropical cyclone relationship was largely based on persistence. Wet years in the Sahel are usually followed by wet years and vice versa. Landsea and Gray (1992) hypothesized that enhanced rainfall in West Africa during the prior year contributed to a strong monsoon the following year through feedbacks from both soil moisture and evapotranspiration. Increased West African rainfall during a particular year indicates that the 200-mb tropical easterly jet is likely stronger than normal and that the easterly waves moving off the coast of Africa are more likely to be stronger than normal.

Additional predictors were added to the early December statistical forecast scheme since the original methodology was established. These included the strength of the Azores ridge and several measures of ENSO (Gray et al. 2000). Strong high pressure near the Azores enhances trade winds and consequently increases upwelling over the tropical Atlantic. Cooler sea surface temperatures are often associated with higher pressure the following spring, which provides a self-enhancing feedback that keeps the trade winds stronger the following spring and summer. Stronger trades are associated with increased vertical wind shear, providing less favorable conditions for development.

Warm ENSO conditions have been well documented to shift the center of convection in the Pacific eastward and consequently alter the Walker circulation. Outflow from this altered Walker circulation manifests itself in westerly anomalies at upper levels in the western tropical Atlantic. Westerly anomalies enhance tropospheric vertical wind shear in the tropical Atlantic (Gray 1984a; Goldenberg and Shapiro 1996) and consequently inhibit development of intense low-latitude Atlantic basin hurricane activity. These additional predictors added to the hindcast variance explained, but the addition of these predictors did not add skill to the real-time forecasts issued during the 1990s. The recent decade failure of this earlier statistical forecast is largely attributed to the failure of the African rainfall and Atlantic hurricane relationship. Although tropical cyclone activity has increased dramatically since 1994, West Africa has continued to report drought conditions typical of inactive hurricane seasons. At this point, we are not sure if this is a real meteorological change or an artifact of station measurement quality and other factors. Table 1 displays the early-December forecast of hurricane days and hurricane destruction potential (HDP) for 1992–2002 compared to what was observed. Although jackknife hindcast skill for 1950–90 suggested that about 50% of the variance could be explained in real-time forecasts, only 3%–7% of the variance has been explained for hurricane days and HDP since the implementation of this scheme in December 1991. This has been the primary motivation for the research presented in this paper.

The recently completed National Centers for Environmental Prediction–National Center for Atmospheric Research (NCEP–NCAR) reanalysis (Kalnay et al. 1996) provides a wealth of global data for analyzing possible predictors for forecasting Atlantic basin tropical cyclones. Reanalysis data provide daily and monthly data worldwide for many variables, including geopotential height, zonal wind, and sea level pressure. An initial inspection of these reanalysis fields indicated that similar hindcast skill to the original forecast methodology could be obtained with a longer 52-yr dataset

TABLE 2. Climatological summary of seasonal tropical cyclone activity from 1950 to 2002. The largest values for any tropical cyclone parameter are shown in boldfaced print, and the smallest values are in italic. The acronyms of the head of each column are defined in the appendix.

Year	NS	NSD	H	HD	IH	IHD	HDP	NTC	TONS	TOH
1950	13	98.00	11	60.00	**7**	15.50	**200**	**230**	8	8
1951	10	58.00	8	36.00	2	5.00	113	115	6	4
1952	7	40.00	6	23.00	3	4.00	70	93	6	6
1953	14	65.00	6	18.00	3	5.50	50	116	6	6
1954	11	52.00	8	32.00	2	8.50	91	124	6	5
1955	12	83.00	9	47.00	5	13.75	158	188	11	**9**
1956	8	30.00	4	13.00	2	2.25	39	66	5	3
1957	8	38.00	3	21.00	2	5.25	67	82	3	2
1958	10	56.00	7	30.00	4	8.25	94	133	9	7
1959	11	40.00	7	22.00	2	3.75	60	94	2	1
1960	7	30.00	4	18.00	2	9.50	72	92	3	2
1961	11	71.00	8	48.00	6	**20.75**	170	211	8	7
1962	5	22.00	3	11.00	*0*	*0.00*	26	32	1	*0*
1963	9	52.00	7	37.00	2	5.50	103	111	7	5
1964	12	71.00	6	43.00	5	9.75	139	160	8	5
1965	6	40.00	4	27.00	1	6.25	73	82	4	1
1966	11	64.00	7	42.00	3	7.00	121	134	5	2
1967	8	58.00	6	36.00	1	3.25	98	93	5	2
1968	7	27.00	4	10.00	*0*	*0.00*	18	39	2	1
1969	17	83.00	**12**	40.00	3	2.75	110	150	6	5
1970	10	23.00	5	7.00	2	1.00	18	62	4	1
1971	13	63.00	6	29.00	1	1.00	65	91	6	2
1972	*4*	21.00	3	6.00	*0*	*0.00*	14	*27*	*0*	*0*
1973	7	33.00	4	10.00	1	0.25	21	50	4	1
1974	7	32.00	4	14.00	2	4.25	46	72	5	3
1975	8	43.00	6	21.00	3	2.25	53	89	4	4
1976	8	45.00	6	26.00	2	1.00	65	82	2	1
1977	6	*14.00*	5	7.00	1	1.00	19	45	*0*	*0*
1978	11	41.00	5	14.00	2	3.50	40	83	4	2
1979	8	44.00	5	22.00	2	5.75	73	92	5	2
1980	11	60.00	9	38.00	2	7.25	126	129	5	4
1981	11	60.00	7	23.00	3	3.75	63	109	5	4
1982	5	16.00	*2*	6.00	1	1.25	18	35	1	*0*
1983	*4*	*14.00*	3	*4.00*	1	0.25	*8*	31	1	*0*
1984	12	51.00	5	18.00	1	0.75	42	74	3	*0*
1985	11	51.00	7	21.00	3	4.00	61	106	4	4
1986	6	23.00	4	11.00	*0*	*0.00*	25	37	1	*0*
1987	7	37.00	3	5.00	1	0.50	13	46	4	1
1988	12	47.00	5	21.00	3	9.25	81	118	7	4
1989	11	66.00	7	32.00	2	9.75	108	130	8	5
1990	14	66.00	8	27.00	1	1.00	57	98	8	3
1991	8	22.00	4	8.00	2	1.25	22	57	2	*0*
1992	6	39.00	4	16.00	1	3.25	51	64	1	*0*
1993	8	30.00	4	10.00	1	0.75	23	52	4	1
1994	7	28.00	3	7.00	*0*	*0.00*	15	35	3	1
1995	**19**	**121.00**	11	**62.00**	5	11.50	172	222	**15**	**9**
1996	13	78.00	9	45.00	6	13.00	136	192	11	8
1997	7	28.00	3	10.00	1	2.00	25	51	2	1
1998	14	80.00	10	49.00	3	9.25	145	166	7	5
1989	12	77.00	8	43.00	5	15.00	145	185	9	7
2000	14	77.00	8	32.00	3	5.25	85	134	9	6
2001	15	63.00	9	27.00	4	5.00	71	137	6	4
2002	12	54.00	4	11.00	2	2.50	31	80	3	2
Mean	9.7	49.40	6.0	24.70	2.3	5.00	72.8	100.9	5.0	3.2
Median	10.0	46.00	6.0	22.00	2.0	3.90	65.0	92.6	5.0	2.5
Std dev	3.3	23.00	2.4	14.90	1.7	4.80	48.6	52.2	3.1	2.6

(1950–2001). In addition, the model utilized to compute the reanalysis data was frozen at the time of the calculations, and therefore so-called climate shifts that are observed to occur when models incorporate new physics are not a factor in the reanalysis.

The focus of this paper now turns to improving the early-December statistical forecast for the following year's tropical cyclone activity in the Atlantic. Section 2 looks at the climatology of a typical hurricane season from 1950–2002, and section 3 elucidates the meth-

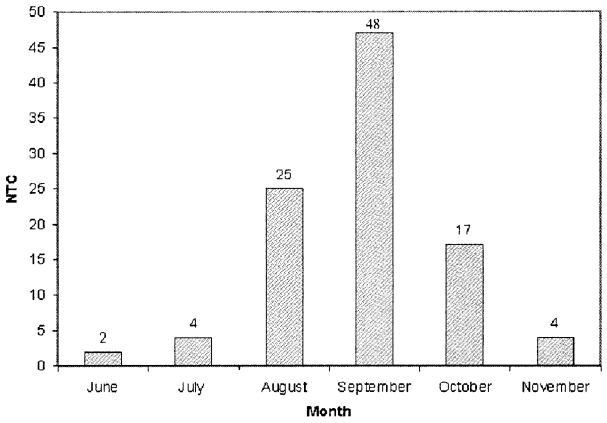

FIG. 1. Net tropical cyclone activity in the Atlantic basin by month (1950–2000).

odology used to develop the updated seasonal forecast. The results of the updated prediction scheme are discussed in section 4, and physical linkages between the predictors and tropical cyclone activity are explained in section 5. Statistical significance is assessed in section 6, and a U.S. landfall probability forecast is outlined in section 7. Conclusions and future work are presented in section 8.

2. Seasonal climatology

The Atlantic basin tropical cyclone season officially runs from 1 June to 30 November, and during this time an average of 9.6 named storms, 5.9 hurricanes, and 2.3 intense hurricanes occur, based on a 1950–2000 climatology. Although the Atlantic hurricane season lasts for 6 months, 95% of all intense tropical cyclones occur between August and October (Landsea 1993). Table 2 displays seasonal tropical cyclone statistics from 1950–2002 according to the Atlantic ''best track'' dataset from the National Hurricane Center. Definitions of the acronyms used in the table are listed in the appendix. A parameter that will be frequently used throughout the rest of this paper is net tropical cyclone (NTC) activity. NTC is an aggregate measure of the following six parameters normalized by their climatological averages: named storms (NS), named storm days (NSD), hurricanes (H), hurricane days (HD), intense hurricanes (IH), and intense hurricane days (IHD). Average annual NTC is 100 by definition. Intense hurricanes prior to 1970 were required to have reached an intensity of 105 kt (versus 100 kt after 1970) due to the overestimation bias discussed in Landsea (1993). Figure 1 displays the NTC activity by month. September is the most active month of an average season followed by August and then October.

Tropical-only named storms (TONS) and tropical-only hurricanes (TOH) are listed in the final two columns of Table 2. Classification of hurricanes as tropical-only hurricanes was discussed in extensive detail in Hess et al. (1995) and Elsner et al. (1996). In general, tropical-only hurricanes develop south of 25°N and originate from Africa-spawned easterly waves. Tropical-only named storms have a similar definition, and their classification is detailed in Blake (2002). Storms that de-

TABLE 3. U.S. landfalling storms by category from 1950 to 2002. The largest values for number of landfalling named storms hurricanes, and intense hurricanes are in boldfaced print.

Year	NS	H	IH
1950	3	3	2
1951	1	0	0
1952	2	1	0
1953	7	3	0
1954	6	5	**3**
1955	5	3	2
1956	2	1	0
1957	5	1	1
1958	1	0	0
1959	7	3	1
1960	5	4	2
1961	3	1	1
1962	0	0	0
1963	1	1	0
1964	5	4	1
1965	3	2	2
1966	2	2	0
1967	2	1	1
1968	4	1	0
1969	3	2	1
1970	3	1	1
1971	5	3	0
1972	3	2	0
1973	1	0	0
1974	1	1	1
1975	1	1	1
1976	2	1	0
1977	1	1	0
1978	2	0	0
1979	6	4	1
1980	2	1	1
1981	3	0	0
1982	1	0	0
1983	3	1	1
1984	2	1	1
1985	**9**	**7**	**3**
1986	2	2	0
1987	2	1	0
1988	3	1	0
1989	3	3	1
1990	1	0	0
1991	1	1	0
1992	3	2	2
1993	2	1	0
1994	4	0	0
1995	6	3	1
1996	3	2	1
1997	1	1	0
1998	7	3	0
1999	5	3	1
2000	2	0	0
2001	3	0	0
2002	7	1	0
Mean	3.2	1.6	0.6
Median	3.0	1.0	0.0
Std dev	2.0	1.5	0.8

TABLE 4. Cross correlations between tropical cyclone parameters.

	NS	NSD	H	HD	IH	IHD	HDP	NTC	TONS	TOH
NS	—	0.87	0.82	0.70	0.63	0.48	0.64	0.78	0.79	0.68
NSD	0.87	—	0.88	0.91	0.75	0.69	0.87	0.92	0.88	0.83
H	0.82	0.88	—	0.87	0.71	0.61	0.83	0.87	0.77	0.79
HD	0.70	0.91	0.87	—	0.77	0.80	0.98	0.94	0.81	0.81
IH	0.63	0.75	0.71	0.77	—	0.85	0.82	0.91	0.74	0.86
IHD	0.48	0.69	0.61	0.80	0.85	—	0.88	0.89	0.72	0.80
HDP	0.64	0.87	0.83	0.98	0.82	0.88	—	0.96	0.80	0.83
NTC	0.78	0.92	0.87	0.94	0.91	0.89	0.96	—	0.87	0.90
TONS	0.79	0.88	0.77	0.81	0.74	0.72	0.80	0.87	—	0.90
TOH	0.68	0.83	0.79	0.81	0.86	0.80	0.83	0.90	0.90	—
Average cross correlation	0.71	0.84	0.79	0.86	0.80	0.78	0.87	0.91	0.81	0.84

veloped into tropical storms from easterly waves but had help from baroclinic influences (i.e., front, cold low) to develop into hurricanes would be classified as a TONS but not a TOH. As was found in Hess et al. (1995), it is generally easier to make seasonal forecasts of tropical cyclones that developed from tropical-only origins than to make seasonal forecasts of high-latitude tropical cyclones.

Landfalling tropical cyclones along the U.S. coastline are a common occurrence, with at least one cyclone of tropical storm intensity making landfall in every year since 1950 except 1962. Twenty-four category 1–2 hurricanes and 16 intense (category 3–4–5) hurricanes have also made landfall between 1950 and 2002. Table 3 lists the number of landfalling storms by intensity for 1950–2002. Please note that if a storm made landfall at two distinct locations, for example Hurricane Andrew (southeast Florida and south-central Louisiana), it was counted as two storms. Two or more intense hurricanes making landfall during any particular year occurs quite infrequently, only happening seven times in the past 53 yr.

Relationships between individual tropical cyclone parameters are shown in a cross-correlation matrix (Table 4). Although there are strong interrelationships between most hurricane parameters, some do not cross correlate as strongly. For example, a perfect knowledge of the number of named storms explains less than 25% of the variance in intense hurricane days. Therefore, it is not surprising that a different group of predictors is used to forecast these two tropical cyclone parameters.

3. Methodology

The early-December statistical forecast scheme attempts to maximize the hindcast skill in forecasting tropical cyclone activity based on the time period 1950–2001. Hindcasting involves selecting predictors

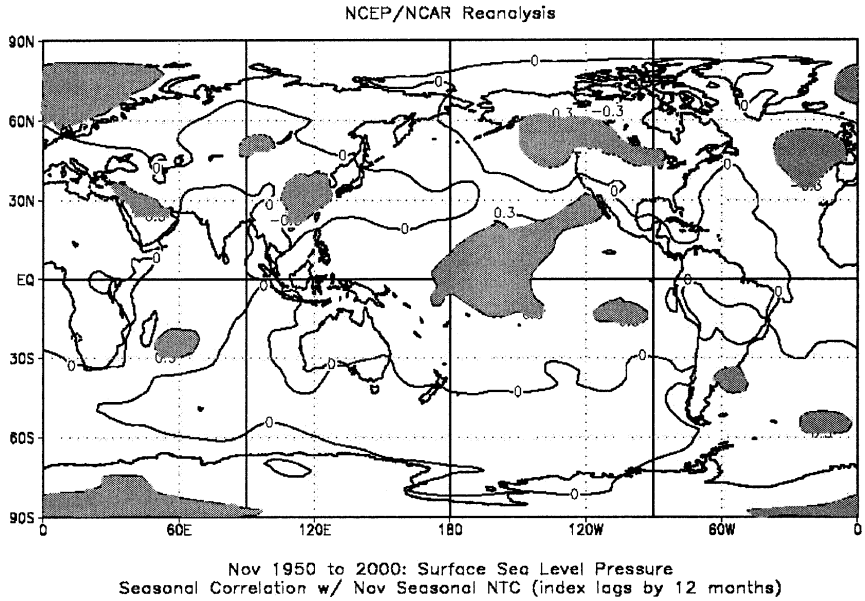

FIG. 2. Correlation map between seasonal NTC and the previous year's Nov sea level pressure. Areas shaded in gray correlated at ($r > |0.3|$).

TABLE 5. Predictors used in the early-Dec forecast. The sign of the predictor associated with increased tropical cyclone activity the next year is in parentheses.

Predictor name	Location
1) Nov 500-mb geopotential height in the far North Atlantic (+)	(67.5°–85°N, 10°E–50°W)
2) Oct–Nov SLP in the Gulf of Alaska (−)	(45°–65°N, 120°–160°W)
3) Sep 500-mb geopotential height in western North America (+)	(35°–55°N, 100°–120°W)
4) Jul 50-mb Equatorial zonal wind (−)	(5°S–5°N, all longitudes)
5) Sep–Nov SLP in the Gulf of Mexico–Southeastern U.S. (−)	(15°–35°N, 75°-95°W)
6) Nov SLP in the tropical northeast Pacific (+)	(7.5°–22.5°N, 125°–175°W)

that were useful in forecasting tropical cyclone activity during the period being hindcast. The forecast model operates on the premise that predictors that hindcast tropical cyclone activity accurately in the past will also be useful for forecasting tropical cyclone activity in the future. The process of obtaining predictors began by seeing what the September–November period looked like in the year prior to an active or inactive year. As mentioned previously, NCEP–NCAR reanalysis data was used as the primary dataset, and composites were constructed using the Climate Diagnostic Center's ''Monthly/Seasonal Climate Composites'' Web page (http://www.cdc.noaa.gov/cgi-bin/Composites/printpage.p1). September, October, and November were composited individually and grouped together to see what atmospheric and oceanic features prevailed in the years prior to the 10 most active and 10 most inactive years. NTC was the tropical cyclone parameter utilized to classify years.

Several features that became evident from the composite maps were anomalously high heights in northern latitudes, indicating a negative Arctic Oscillation (AO) (Thompson and Wallace 1998) and North Atlantic Oscillation (NAO) (van Loon and Rogers 1978) and a midlatitude wave train pattern closely resembling a positive and slightly eastward-shifted Pacific–North American pattern (PNA) (Wallace and Gutzler 1981). A positive PNA is a typical wintertime midlatitude teleconnection associated with warm ENSO conditions (Horel and Wallace 1981), and the eastward shift of the PNA is likely due to an eastward shift of sea surface temperature anomalies from the central to the east Pacific. A wave train propagates poleward and eastward from an area of thermal forcing (Hoskins and Karoly 1981), and therefore, if the warmest temperature anomalies were located in the eastern Pacific, the Pacific North American pattern would also be shifted eastward. In general, warm temperatures in the east Pacific are more unstable than in the central Pacific and are therefore more likely to shift back to neutral or cool conditions the following year.

The primary tool used in selecting predictors was the Climate Diagnostic Center's ''Linear Correlations'' Web page (http://www.cdc.noaa.gov/Correlation) which allowed for testing correlations between global data fields and TC activity time series created by the user, such as NTC. Correlations between atmospheric data fields and Atlantic basin tropical cyclone activity indices were calculated. Figure 2 shows the correlation between the following year's NTC and November sea level pressure. Other predictors in the scheme were selected utilizing a residual. For this, one or two predictors already in the forecast model were used to predict the TC variable in question, for example, NTC. The difference between actual value minus hindcast value for each year was considered the hindcast error, and a time series of these hindcast errors was created. Correlation maps between these residual time series and global atmospheric and oceanic features were then constructed to see if there were any large-scale areas that correlated strongly with

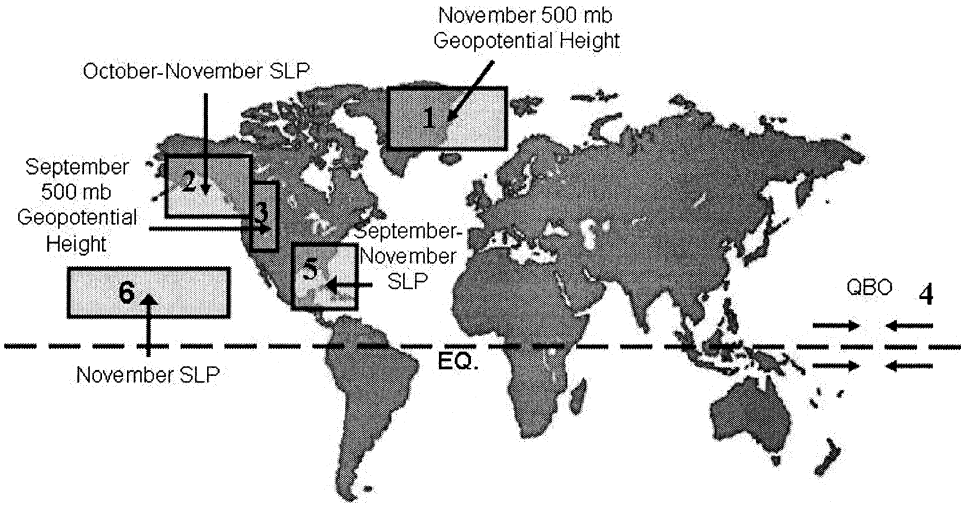

FIG. 3. Map of predictors used in the early-Dec statistical forecast.

TABLE 6. Predictors chosen, hindcast variance explained, and jackknife variance explained for each TC activity parameter in the early-Dec forecast of the next year's tropical cyclone activity. See Table 5 for predictor names and descriptions.

Forecast parameter	No. of predictors	Predictors chosen from table	Variability explained by hindcast (r^2) (1950–2001)	Likely independent forecast skill (jackknife)
NS	3	1, 2, 3	0.40	0.29
NSD	5	1, 3, 4, 5, 6	0.45	0.28
H	5	1, 2, 3, 4, 5	0.53	0.38
HD	5	1, 2, 3, 4, 5	0.53	0.35
IH	5	1, 2, 3, 4, 5	0.69	0.57
IHD	5	1, 3, 4, 5, 6	0.51	0.41
HDP	5	1, 3, 4, 5, 6	0.57	0.37
NTC	5	1, 3, 4, 5, 6	0.62	0.46
TONS	4	1, 4, 5, 6	0.44	0.30
TOH	5	1, 3, 4, 5, 6	0.59	0.43

both the residual and the predictand itself. September 500-mb geopotential height over the western United States and the QBO predictor were selected based on the residual approach. In addition, all predictors selected were required to span an area no less than 10° by 20° in extent to avoid local ''bull's-eye'' features that are prevalent on some of the correlation maps.

4. Results

Nineteen predictors were evaluated for potential forecasting ability, and six predictors spanning various portions of the globe were selected to forecast Atlantic basin tropical cyclones using the methodology outlined in the previous section. Predictors utilize zonal wind, sea level pressure, or geopotential height data that are defined in Kalnay et al. (1996) to be reanalysis ''A'' variables. These variables are primarily observation-driven and are therefore considered to be the most accurate in the reanalysis dataset. Table 5 lists the locations of the six predictors, and Fig. 3 displays these predictors on a map. A listing of predictors chosen for forecasting each tropical cyclone activity parameter along with the variance explained and the cross-validated or jackknifed variance explained are listed in Table 6. Jackknife or cross-validated variance explained is calculated utilizing the technique outlined in Elsner and Schmertmann (1994). This methodology examines how well a year can be predicted using data that are independent of the year being forecast. Each of the 52 years in the dataset were predicted utilizing an equation developed on the remaining 51 yr of data. For example, a forecast for 1950 would be based on an equation developed on the years 1951–2001. Jackknifed hindcast skill gives a more accurate representation of actual forecast conditions and is often considered to be an upper bound on how much variance will likely be explained by the scheme when forecasts are issued in real time.

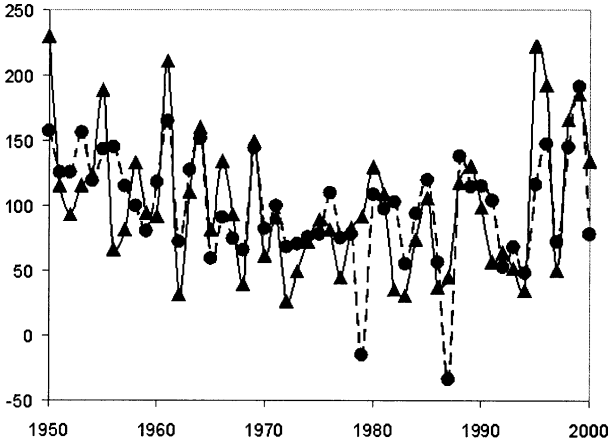

FIG. 4. Actual NTC (solid line) vs early-Dec cross-validated hindcast NTC (dashed line). Cross-validated variance (r^2) explained is 0.46.

More intense tropical cyclone parameters tended to be better forecast than parameters dealing with weaker systems. For example, there was a nearly 30% better cross-validated hindcast variance explained for intense hurricanes compared to named storms. This result is to be expected since weaker systems often form from higher-latitude baroclinically generated disturbances that are impossible to predict months in advance, such as frontal boundaries or cold lows. Also, there are more observational problems in determining the intensity of the weaker systems.

Predictors were selected using an all-subset technique similar to that used in Klotzbach and Gray (2003). This procedure is different from stepwise regression in that it selects the best one predictor, the best two predictors, etc., up to the best five predictors for each tropical cyclone variable or until the jackknifed hindcast skill no longer increases. No more than five predictors were selected for each TC parameter to avoid statistical overfitting of the data. An ordinary least squares multiple regression technique was utilized for most predictands, but a Poisson regression model was utilized for tropical cyclone predictands that frequently have small integer values, as suggested by Elsner and Schmertmann (1993). Please refer to the above paper for a more complete description of the Poisson model. For the seasonal forecast, a Poisson model was implemented for IH,

TABLE 7. Observed NTC, early-Dec cross-validated hindcast NTC, hindcast residual, and residual assuming a climatological NTC forecast of 100. The average residual is computed without respect to sign.

Year	Observed NTC	Hindcast NTC	Hindcast error	Error using climatology
1950	230	157	73	130
1951	115	125	−10	15
1952	93	126	−33	−7
1953	116	156	−40	16
1954	124	119	5	24
1955	188	143	45	88
1956	66	145	−79	−34
1957	82	115	−33	−18
1958	133	100	33	33
1959	94	80	14	−6
1960	92	118	−26	−8
1961	211	165	46	111
1962	32	72	−40	−68
1963	111	127	−16	11
1964	160	151	9	60
1965	82	60	22	−18
1966	134	91	43	34
1967	93	74	19	−7
1968	39	66	−27	−61
1969	150	144	6	50
1970	62	82	−20	−38
1971	91	99	−8	−9
1972	27	68	−41	−73
1973	50	71	−21	−50
1974	72	76	−4	−28
1975	89	78	11	−11
1976	82	110	−28	−18
1977	45	75	−30	−55
1978	83	78	5	−17
1979	92	−15	107	−8
1980	129	108	21	29
1981	109	97	12	9
1982	35	102	−67	−65
1983	31	55	−24	−69
1984	74	94	−20	−26
1985	106	120	−14	6
1986	37	56	−19	−63
1987	46	−34	80	−54
1988	118	138	−20	18
1989	130	114	16	30
1990	98	115	−17	−2
1991	57	104	−47	−43
1992	64	53	11	−36
1993	52	68	−16	−48
1994	35	48	−13	−65
1995	222	116	106	122
1996	192	147	45	92
1997	51	72	−21	−49
1998	166	145	21	66
1999	185	191	−6	85
2000	134	78	56	34
2001	129	123	6	29
Average error			|30|	|41|

TABLE 8. Observed NTC, early-Dec cross-validated hindcast NTC, hindcast error, and error assuming a climatological NTC forecast of 100 units for the bottom 15 and top 15 years, respectively, for observed NTC. Years in which the hindcast NTC was a more accurate forecast than climatology are in boldface. The average error is computed without respect to sign.

Year	Observed NTC	Hindcast NTC	Hindcast error	Error using climatology
Bottom 15 years				
1972	27	68	−41	−73
1983	31	55	−24	−69
1962	32	72	−40	−68
1994	35	48	−13	−65
1982	35	102	−67	−65
1986	37	56	−19	−63
1968	39	66	−27	−61
1977	45	75	−30	−55
1987	46	−34	80	−54
1973	50	71	−21	−50
1997	51	72	−21	−49
1993	52	68	−16	−48
1991	57	104	−47	−43
1970	62	82	−20	−38
1992	64	53	11	−36
Average error			|32|	|56|
Top 15 years				
1950	230	157	73	130
1995	222	116	84	122
1961	211	165	46	111
1996	192	147	45	92
1955	188	143	45	88
1999	185	191	−6	85
1998	166	145	21	66
1964	160	151	9	60
1969	150	144	6	50
2001	137	123	14	37
1966	134	91	43	34
2000	134	78	56	34
1958	133	100	33	33
1989	130	114	16	30
1980	129	108	21	29
Average error			|35|	|67|

TONS, and TOH. Since the assumption of equal variances is clearly violated for these predictands, a Poisson model was considered appropriate. In addition, a Poisson model does not allow negative numbers to be forecast for a predictand. This problem was sometimes observed when an ordinary least squares multiple regression equation was utilized for IH, TONS, and TOH.

Figure 4 displays a 52-yr time series of observed versus cross-validated hindcast NTC for 1950–2001, and Table 7 displays actual NTC, cross-validated hindcast NTC, hindcast error, and the error assuming a climatological forecast of 100 NTC for each year. As one can see from Table 7, there is about a 27% reduction in the average residual utilizing the statistical forecast over climatology.

A more powerful case for the importance of this statistical forecast can be seen when examining years with much above-average and much below-average NTC values. For example, as can be seen in Table 8, for the 15 years with the lowest observed NTC (<65 units), the cross-validated statistical hindcast was more successful than a climatological NTC forecast of 100 in 12 out of 15 years. Likewise, for the 15 years with the highest observed NTC (>125 units), the cross-validated statistical hindcast was more accurate than a forecast of cli-

TABLE 9. Observed NTC, early-Dec cross-validated hindcast NTC, hindcast error, and error assuming a climatological NTC forecast of 100 units for the bottom 15 and top 15 years, respectively, for cross-validated hindcast NTC. Years in which the hindcast NTC was a more accurate forecast than climatology are in boldface. The average error is computed without respect to sign.

Year	Observed NTC	Hindcast NTC	Hindcast error	Error using climatology
Bottom 15 years				
1987	46	−34	80	−54
1979	92	−15	107	−8
1994	35	48	−13	−65
1992	64	53	11	−36
1983	31	55	−24	−69
1986	37	56	−19	−63
1965	82	60	22	−18
1968	39	66	−27	−61
1993	52	68	−16	−48
1972	27	68	−41	−73
1973	50	71	−21	−50
1962	32	72	−40	−68
1997	51	72	−21	−49
1967	93	74	19	−7
1977	45	75	−30	−55
Average error			|33|	|48|
Top 15 years				
1999	185	191	−6	85
1961	211	165	46	111
1950	230	157	73	130
1953	116	156	−40	16
1964	160	151	−9	60
1996	192	147	45	92
1998	166	145	21	66
1956	66	145	−79	−34
1969	150	144	6	50
1955	188	143	45	88
1988	118	138	−20	18
1963	111	127	−16	11
1952	93	126	−33	−7
1951	115	125	−10	15
2001	137	123	14	37
Average error			|31|	|55|

matology in 13 out of 15 years. Another way to consider the success of the statistical forecast is to examine years in which hindcast NTC was much above average or much below average (Table 9). In the 15 years with the lowest cross-validated hindcast NTC (<75 units), the hindcast was a better forecast than climatology in 11 out of 15 years, and in all 15 years, observed NTC was below average. For the 15 years with the highest cross-validated hindcast NTC (>122 units), the hindcast was a better forecast than climatology in 10 out of 15 years, and in 13 out of 15 years, observed NTC was above average. These examples serve to illustrate that, although the hindcast showed little skill in average years (years with small deviations from climatology), in years with large deviations from climatology, the hindcast was a better forecast than climatology over 80% of the time and was able to determine the right direction from climatology nearly 95% of the time. These results are es-

TABLE 10. Early-Dec old and new statistical forecasts and observed values of hurricane days and hurricane destruction potential for 1992–2002. The average difference between forecast and observed values was taken without respect to sign.

Year	Old forecast hurricane days	New forecast hurricane days	Observed hurricane days	Old difference	New difference	Old forecast hurricane destruction potential	New forecast hurricane destruction potential	Observed hurricane destruction potential	Old difference	New difference
1992	15	9	16	−1	−7	35	23	51	−16	−28
1993	25	19	10	15	9	75	53	23	52	30
1994	25	8	7	18	1	85	16	15	70	1
1995	35	35	62	−27	−27	100	115	173	−73	−58
1996	20	34	45	−25	−11	50	103	135	−85	−32
1997	25	21	10	15	11	75	60	26	49	34
1998	20	32	49	−29	−17	50	99	145	−95	−46
1999	40	45	43	−3	2	130	146	145	−15	1
2000	25	18	32	−7	−14	85	51	85	0	−34
2001	20	27	27	−4	0	65	81	71	−6	10
2002	35	29	11	24	18	90	93	31	59	62
Average difference				|15.3|	|10.6|				|47.3|	|30.5|
R^2				0.05	0.52				0.03	0.58
Jackknife hindcast R^2 (1950–90)				0.51	0.46				0.53	0.50

TABLE 11. Correlations between individual predictors for the Dec forecast. Most intercorrelations are below $r = |0.3|$. Average intercorrelations are computed without respect to sign. See Table 5 for predictor names and descriptions.

Predictor	1	2	3	4	5	6
1	—	−0.24	0.04	−0.14	−0.27	0.19
2	−0.24	—	−0.29	0.24	0.21	−0.57
3	0.04	−0.29	—	−0.07	−0.13	0.13
4	−0.14	−0.24	−0.07	—	0.09	0.01
5	−0.27	0.21	−0.13	0.09	—	−0.12
6	0.19	−0.57	0.13	0.01	−0.12	—
Average intercorrelation	0.18	0.31	0.13	0.11	0.16	0.20

pecially impressive considering that the hindcast was issued 6 months before the beginning of the hurricane season.

Table 10 examines the improvement of the new statistical forecast over the old statistical forecast for the years 1992–2002. The old statistical forecast was developed on hindcast data from 1950–90 and was first issued operationally in December 1991, but, although the scheme showed significant skill in hindcast mode, it has shown little skill in forecast mode. For this comparison, the forecasts for the new scheme were also developed on the hindcast years of 1950–90. The new scheme explains approximately the same amount of variance during the 1992–2002 period as it did during the hindcast period compared with the complete failure of the earlier scheme during this same period. The average residual was reduced by about 30%–35% for hurricane days and HDP when using the new statistical scheme over the 1992–2002 period.

Table 11 displays a cross-correlation matrix between all predictors in the early December statistical forecast scheme. All correlations are below $r = |0.3|$ except for the relationship between the Gulf of Alaska October–November sea level pressure (SLP) and the November SLP in the tropical northeast Pacific. According to a two-tailed Student's t test, 95% and 99% significance levels of interrelationships between predictors are 0.28 and 0.36, respectively. Obtaining predictors that are mostly uncorrelated with each other is valuable in that each predictor provides mostly independent information from the other predictors in the scheme.

5. Physical links between predictors and seasonal tropical cyclone activity in the Atlantic basin

Many of the predictors selected for forecasting the following year's tropical cyclone activity were not previously known to be related to current or future hurricane activity in the Atlantic basin; however, in combination with the other predictors in the forecast scheme, they were able to explain 46% of the cross-validated hindcast variance in Atlantic basin NTC activity 6–11 months in advance. One would not have expected the atmosphere–ocean to have such a long-term memory for the frequency of mesoscale events.

One way to better understand the predictors in the

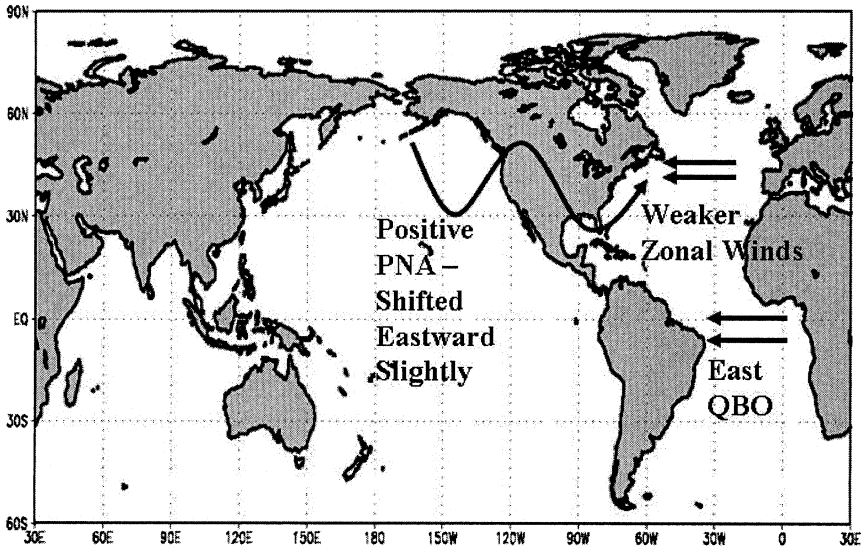

FIG. 5. Summer–fall atmospheric features associated with an active hurricane season the following year.

TABLE 12. Correlations between predictors and Atlantic tropical cyclone activity parameters. Correlations that exceed the 95% significance level as determined by the Student's *t* test are in italics, those that exceed the 99% significance level as determined by the Student's *t* test are in bold and those not significant at the 95% level are underlined. See Table 5 for predictor names and descriptions.

Predictor	NS	NSD	H	HD	IH	IHD	HDP	NTC	TONS	TOH
1	**0.50**	**0.48**	**0.52**	**0.51**	**0.57**	*0.47*	**0.51**	**0.57**	*0.45*	**0.49**
2	*−0.45*	*−0.44*	**−0.53**	**−0.48**	**−0.49**	−0.42	**−0.48**	**−0.52**	−0.39	**−0.48**
3	*0.30*	0.31	0.31	0.35	0.41	0.40	0.39	0.40	0.31	0.40
4	*−0.25*	−0.27	−0.19	−0.27	−0.33	−0.29	−0.31	−0.31	−0.22	−0.28
5	*−0.29*	−0.32	*−0.43*	*−0.45*	−0.32	−0.39	*−0.47*	−0.41	−0.40	−0.42
6	*0.36*	0.40	0.34	0.35	0.36	0.37	0.35	0.40	0.37	*0.44*

statistical forecast is to investigate the physical relationships between each predictor and tropical cyclone activity the following year. A method used to understand physical relationships between predictors and tropical cyclone activity was to correlate each predictor with other atmospheric fields during the month that the predictor is selected along with atmospheric fields during the following year's August–October period. By doing this, one can see global effects that occur concurrently with the predictor and also the teleconnected effects that happen 6–11 months later. These correlation maps were helpful in establishing the physical relationships discussed in the following paragraphs. For example, Fig. 5 displays three fall features that were usually associated with an active hurricane season the following year. A discussion of hypothetical physical linkages between each of the predictors in the scheme and Atlantic basin tropical cyclone activity follows.

a. Predictor 1: November 500-mb geopotential height in the far North Atlantic (67.5°–85°N, 10°E–50°W) (+)

Positive values of this predictor correlate very strongly ($r = -0.7$) with negative values of the AO and the NAO. Negative AO and NAO values imply more ridging in the central Atlantic and a warm North Atlantic Ocean (50°–60°N, 10°–50°W) due to stronger southerly winds during this period. Also, on decadal time scales, weaker zonal winds in the subpolar areas (40°–60°N, 0°–60°W) across the Atlantic are indicative of a relatively strong thermohaline circulation. The change in strength of the zonal winds at 500 mb from the period inferred to have an active thermohaline circulation (1950–69, 1995–99) from the period inferred to have a weak thermohaline circulation (1970–94) was found to be statistically significant at the 99% level. Also, positive values of this November index (higher heights, weaker midlatitude zonal winds) are correlated with weaker tropical Atlantic 200-mb westerly winds and weaker trade winds the following August–October. The associated reduced tropospheric vertical wind shear enhances TC development. Other following summer–early fall features that are directly correlated with this predictor are low sea level pressure in the Caribbean and a warm North and tropical Atlantic. Both of the latter are hurricane-enhancing factors.

b. Predictor 2: October–November SLP in the Gulf of Alaska (45°–65°N, 120°–160°W) (−)

Negative values of this predictor are strongly correlated with a positive ''Alaskan pattern'' (Renwick and Wallace 1996) as well as a slightly eastward-shifted positive PNA, which implies reduced ridging over the central Pacific with increased heights over the western United States. The negative mode of this predictor is typically associated with warm-current eastern Pacific equatorial SST conditions and a mature warm ENSO event. Low sea level pressure is observed to occur in the Gulf of Alaska with a decaying El Niño event, and anomalously high pressure is observed with a weakening La Niña event (Larkin and Harrison 2002). Negative values of this predictor indicate a likely change to cool ENSO conditions the following year. Cool ENSO conditions enhance Atlantic hurricane activity.

TABLE 13. Miller equivalent F test results for the early-Dec forecast equations.

Predictor	Miller F_{99}	52-yr F value	Significant 99% level
NS	6.93	10.81	Yes
NSD	5.31	7.66	Yes
H	5.31	10.52	Yes
HD	5.31	9.96	Yes
IH	5.31	12.75	Yes
IHD	5.31	9.40	Yes
HDP	5.31	12.03	Yes
NTC	5.31	14.90	Yes
TONS	5.94	8.17	Yes
TOH	5.31	12.27	Yes

TABLE 14. Correlations between NTC and forecast predictors subdivided into 1950–69 and 1975–94. See Table 5 for predictor names and descriptions.

Predictor	1950–69 correlation	1975–94 correlation	1950–2000 correlation	Correlation difference
1	0.45	0.25	0.57	0.20
2	−0.57	−0.52	−0.52	0.05
3	0.29	0.25	0.40	0.04
4	−0.65	−0.23	−0.31	0.42
5	−0.24	−0.48	−0.41	0.24
6	0.32	0.43	0.40	0.11

TABLE 15. Ratio of top 10–bottom 10 years for all predictors in the early-Dec forecast scheme. See Table 5 for predictor names and descriptions.

Predictor	NS	NSD	H	HD	IH	IHD	HDP	NTC	TONS	TOH	Mean
1	1.61	1.86	1.68	2.27	3.58	3.56	2.48	2.30	2.39	3.44	2.52
2	1.52	1.70	1.72	2.05	2.82	3.75	2.32	2.09	2.06	3.92	2.40
3	1.52	1.63	1.59	1.78	2.50	2.27	2.01	1.81	1.97	3.60	2.07
4	1.19	1.28	1.17	1.32	1.65	1.53	1.40	1.35	1.39	1.70	1.40
5	1.22	1.46	1.54	2.09	1.76	3.13	2.36	1.75	2.37	3.13	2.08
6	1.35	1.63	1.46	1.71	1.88	2.53	1.83	1.72	1.86	2.78	1.87
Mean	1.40	1.59	1.52	1.87	2.37	2.80	2.07	1.84	2.01	3.10	2.06

c. Predictor 3: September 500-mb geopotential height in western North America (35°–55°N, 100°–120°W) (+)

Positive values of this predictor correlate very strongly ($r = 0.8$) with positive values of the PNA. PNA values are usually positive in the final year of an El Niño event (Horel and Wallace 1981). Therefore, cooler ENSO conditions are likely during the following year. Significant lag correlations exist between this predictor and enhanced 200-mb geopotential height anomalies in the subtropics during the following summer. Higher heights in the subtropics reduce the height gradient between the deep Tropics and subtropics, resulting in easterly anomalies at 200 mb throughout the tropical Atlantic during the following summer. Easterly anomalies at 200 mb provide a strong enhancing factor for tropical cyclone activity.

d. Predictor 4: July 50-mb equatorial zonal wind (5°S–5°N, all longitudes) (−)

Easterly anomalies of the QBO during the previous July indicate that the QBO will likely be in the west phase during the following year's hurricane season. According to Gray et al. (1992a), the average half-period of the QBO lasts approximately 14 months (average period 28–29 months). The QBO should therefore be of opposite sign during the following year's August–October period. The west phase of the QBO has been shown to provide favorable conditions for the development of hurricanes in the deep Tropics, as discussed by Shapiro (1989) and Gray et al. (1992a, 1993, 1994). Hypothetical mechanisms for how the QBO affects hurricanes are as follows: (a) Atlantic TC activity is inhibited during easterly phases of the QBO due to enhanced lower-stratospheric wind ventilation and increased upper-troposphere–lower-stratosphere wind shear; (b) the east phase of the QBO favors equatorial convection (0°–10°N), and the west phase of the QBO favors higher-latitude convection (10°–20°N), which is more favorable for TC development; and (c) the west phase of the QBO has a slower relative wind (advective wind relative to the moving system) than does the east phase (Gray and Sheaffer 1991). This allows for greater coupling between the lower stratosphere and the troposphere, which is an enhancing factor for Atlantic basin tropical cyclone activity.

e. Predictor 5: September–November SLP in the Gulf of Mexico–southeastern United States (15°–35°N, 75°–95°W) (−)

Low pressure in this area during September–November correlates quite strongly with a current positive phase of the PNA. As was stated earlier, the PNA is usually positive in the final year of an El Niño event, and therefore cooler ENSO conditions are likely the following year (Horel and Wallace 1981). This feature is strongly negatively correlated ($r \sim -0.5$) with the following year's August–September sea level pressure in the tropical and subtropical Atlantic. August–September SLP in the tropical Atlantic is one of the most important predictors for seasonal activity; that is, lower-than-normal sea level pressure is favorable for more TC activity. Easterly anomalies at 200 mb are also typical

TABLE 16. Correlation of the previous year's Jul–Nov period for the Gulf of Mexico–southeastern U.S. predictor with the following year's seasonal NTC.

Month	Correlation
Jul	−0.33
Aug	−0.26
Sep	−0.42
Oct	−0.20
Nov	−0.14
Average correlation	−0.23

TABLE 17. Entire U.S. number of landfalling tropical cyclones for the top 15 and bottom 15 years of cross-validated hindcast NTC + SSTA* (top) and for the top 15 and bottom 15 years of observed NTC + SSTA* (bottom), respectively.

Hindcast landfall occurrences	NS	H	IH
15 highest NTC + SSTA*	65	37	15
15 lowest NTC + SSTA*	3	16	7
Ratio (as percentage)	197	231	214
Observed landfall occurrences	NS	H	IH
15 highest NTC + SSTA*	62	34	12
15 lowest NTC + SSTA*	28	15	6
Ratio (as percentage)	221	227	200

TABLE 18. Gulf Coast number of landfalling tropical cyclones for the top 15 and bottom 15 years of cross-validated hindcast NTC + SSTA* (top) and for the top 15 and bottom 15 years of observed NTC + SSTA* (bottom), respectively.

Hindcast landfall occurrences	NS	H	IH
15 highest NTC + SSTA*	31	13	5
15 lowest NTC + SSTA*	18	9	5
Ratio (as percentage)	172	144	100
Observed landfall occurrences	NS	H	IH
15 highest NTC + SSTA*	32	14	6
15 lowest NTC + SSTA*	14	8	4
Ratio (as percentage)	229	175	150

TABLE 19. East Coast number of landfalling tropical cyclones for the top 15 and bottom 15 years of cross-validated hindcast NTC + SSTA* (top) and for the top 15 and bottom 15 years of observed NTC + SSTA* (bottom), respectively.

Hindcast landfall occurrences	NS	H	IH
15 highest NTC + SSTA*	34	24	10
15 lowest NTC + SSTA*	15	7	2
Ratio (as percentage)	227	343	500
Observed landfall occurrences	NS	H	IH
15 highest NTC + SSTA*	31	22	6
15 lowest NTC + SSTA*	14	7	2
Ratio (as percentage)	221	314	300

during the following year's August–October period, with low values of this predictor.

f. Predictor 6: November SLP in the tropical northeast Pacific (7.5°–22.5°N, 125°–175°W) (+)

According to Larkin and Harrison (2002), high pressure in the tropical northeast Pacific appears during most winters preceding the development of a La Niña event. High pressure forces stronger trade winds in the east Pacific, which increases upwelling and helps initiate La Niña conditions, which eventually enhance Atlantic hurricane activity during the following summer. This predictor correlates with low geopotential heights at 500 mb throughout the Tropics the following summer, indicative of a weaker Hadley circulation typical of La Niña conditions. Also, high pressure in November in the tropical northeast Pacific correlates with low sea level pressure in the tropical Atlantic and easterly anomalies at 200 mb during the following August–October period.

The predictors discussed in detail above all relate to one or more of five global modes: the NAO, the AO, the PNA, ENSO, and the QBO. With a knowledge of the current value and a forecast of the future trends in these modes, one can explain up to about half of the variance of the following year's tropical cyclone activity based on 52 yr of hindcast data.

6. Statistical analysis of predictors

The last section proposed physical linkages between predictors and Atlantic basin tropical cyclone activity. Another method used to add credibility to the forecast scheme is to use objective statistical bootstrap techniques to show that the predictors have statistically significant following-year correlations with tropical cyclone activity over the 52-yr developmental dataset period. One of the most common methods of evaluating statistical significance is to utilize a standard Student's *t* test. The QBO was expected to relate to Atlantic tropical cyclones (Gray 1984a,b; Shapiro 1989); however, all other areas were selected utilizing the correlation and composite analysis. These areas were selected a posteriori; that is, the relationship was not expected prior to the forecast development, and therefore each region must pass a two-tailed test. For all predictors, the actual significance level needed is computed by taking the desired significance level and raising it to the number of potential predictors in the scheme (19 potential predictors). To obtain the 95% significance level, one must calculate the value that when taken to the 19th power will give you 0.95 (Wilks 1995). Utilizing this information in the *t* test, the 95% significance level for all predictors except the QBO is 0.43, and the 99% significance level is 0.48. Since the QBO relationship was already expected, the 95% and 99% significance levels for this relationship are reduced to 0.39 and 0.45, respectively. Table 12 displays correlations between all predictors and Atlantic TC parameters. Predictors 1 and 2 show the highest correlation with Atlantic TC activity the following year. Predictors 3 and 4 were selected from the residual analysis, and therefore it is expected that the individual correlations between the predictors and TC parameters are weakest for these features. It should also be noted that the power of this forecasting scheme does not lie simply in the strength of the individual predictors but in the strength of the predictors when used in combination.

A method used to check the statistical significance of the forecast equation as a whole is the Miller equivalent F test (Neumann et al. 1977). An ordinary F test would overestimate the statistical significance, since 19 predictors were evaluated for possible use in this scheme. Therefore, to calculate the actual F value needed for statistical significance, the total number of variables must be considered. Therefore, the 99% significance level proposed by Miller is as follows:

$$F_{99} = F_{(1-1/100k)}, \quad (1)$$

where k is the number of predictors screened for use in the forecast. Since 19 predictors were considered, the actual F value needed for 99% significance is $F_{0.99947}$. Table 13 displays the calculated F values needed for 99% significance based on Eq. (1) along with the actual F values for the individual forecast equations based on

52 yr of hindcasting. All forecast equations are significant at the 99% level.

Another way to evaluate statistical significance is to investigate the stability of the correlations. By evaluating periods of time when the Atlantic thermohaline circulation was strong and when the thermohaline circulation was weak, one can determine if the predictors are stable throughout the period. Two 20-yr periods were selected for the subdivision of the data. From 1950 to 1969, the Atlantic thermohaline circulation was judged to be strong based on a North Atlantic sea surface temperature proxy, and the Atlantic thermohaline circulation was judged to be weak from 1975 to 1994. Warm North Atlantic sea surface temperatures imply a strong thermohaline circulation, while cold North Atlantic sea surface temperatures imply a weak thermohaline circulation. Table 14 displays correlations between predictors and Atlantic TC parameters for both 1950–69 and 1975–94. In general, correlations were stable throughout both time periods. The two predictors with the most significant correlation changes were the stratospheric QBO predictor and the southeastern U.S. predictor. Since the physical relationship between the QBO and hurricanes has been well documented in the literature (e.g., Gray 1984a; Shapiro 1989; Gray et al. 1992a, 1993, 1994), this predictor will be kept in the predictor pool. The southeastern U.S. predictor will be subjected to a further statistical test to determine its validity in the predictor pool.

An additional test to evaluate the strength of relationships between predictors and Atlantic TC parameters was to evaluate the top 10 and bottom 10 values of each predictor. For example, take the North Atlantic 500-mb geopotential height, and compute a ratio for tropical cyclone activity that occurred during the top 10 versus the bottom 10 of those years. If there was a negative relationship between the predictor and TC activity, the ratio was inverted to allow for easy reference between each predictor–Atlantic TC parameter pair. Table 15 displays the top 10–bottom 10 ratios. Many of the ratios are of greater magnitude than 2:1, indicating significant relationships between the predictor and Atlantic hurricanes.

The Gulf of Mexico–southeastern U.S. predictor, one of the predictors that had a significant change in correlation between the active and inactive thermohaline eras, was subjected to further evaluation. Sea level pressure in this region from July to November of the prior year was correlated with the following year's seasonal NTC value from 1950 to 2001 to see if the negative correlation tended to persist from month to month. Table 16 displays the July–November correlations. All months from July to November show a negative correlation, adding more confidence to the use of the southeastern U.S. area as a predictor. In addition, the eastward-shifted PNA–Atlantic TC relationship discussed in section 5 adds further credence to the selection of this predictor. An eastward-shifted PNA indicates that the warm ENSO conditions are concentrated in the east Pacific. Warmth near the Peruvian coast tends to change from year to year, while warm anomalies near the international date line are much more stable and may persist for several years. Therefore, an El Niño event with warmth in the east Pacific (Niño-1, -2, -3) is much more likely to change to neutral or cool La Niña conditions during the following summer than an El Niño event with warmth concentrated in the central Pacific (Niño-3.4, -4).

7. U.S. landfall probability forecast

One of the most critical aspects of any tropical cyclone forecast is the issuance of landfall probabilities. Previous work has been conducted on the predictability of landfalling hurricanes (Lehmiller et al. 1997; Bove et al. 1998; Elsner et al. 2000), but the issuance of landfall probabilities has not been attempted until recently, by Gray et al. (2000). Although there are only small differences in landfalling tropical storms between individual active and inactive years, there are considerable differences in the number of intense hurricanes that make landfall along the U.S. coastline when one averages 4–5 active years versus 4–5 inactive years. With the upturn in tropical cyclone activity since 1995, the probability of an intense hurricane striking the U.S. coastline has increased accordingly (Goldenberg et al. 2001). For example, during the 15 years with the largest NTC hindcasts, 13 intense hurricanes made landfall along the U.S. coastline as opposed to only 8 intense hurricanes during the 15 least active years. For the U.S. East Coast, this ratio is 10 to 2. The ratios are even more significant along the U.S. East Coast than for the entire United States. The Gulf Coast–East Coast demarcation location is approximately 50 miles north of Tampa, Florida. Storms that make landfall near Tampa, Fort Myers, and the Florida Keys are considered to be East Coast landfalls. During the 15 highest NTC hindcasts, eight intense hurricanes made landfall along the East Coast as opposed to only three intense hurricanes during the 15 lowest NTC hindcasts, or a ratio difference of 2.67:1.

An additional parameter to aid in issuing landfall probabilities, proposed by Gray et al. (2000), is defined as SSTA*. SSTA* is a proxy measure of the strength of the Atlantic thermohaline circulation and is a weighted average measure of sea surface temperature anomalies in the region bounded by 50°–60°N, 10°–50°W. SSTA* is calculated in the following manner:

$$\text{SSTA}^* = \overline{\text{SSTA}}_6 + \frac{1}{2}(\overline{\text{SSTA}}_1) + \frac{1}{4}(\overline{\text{SSTA}}_{2-1}), \quad (2)$$

where SSTA* is the influence of the North Atlantic (50°–60°N, 10°–50°W) SST anomalies on the coming year U.S. tropical cyclone landfall (values are expressed in 10^{-2}°C), $\overline{\text{SSTA}}_6$ is the average mean North Atlantic SST anomaly for the prior 6 yr, $\overline{\text{SSTA}}_1$ is the mean SST anomaly of the last year, and SSTA_{2-1} is last year's July–

November SST anomaly minus last year's January through June anomaly.

As one can see from the equation, SSTA* takes into account North Atlantic sea surface temperatures for the past 6 yr with a heavier weight on SSTs during the past year and 6 months, respectively. SSTA* is closely related to the Atlantic multidecadal mode documented in Goldenberg et al. (2001), whereby a warm Atlantic is positively correlated with more hurricanes and increased likelihood of landfall. The use of the past-6-yr average of North Atlantic sea surface temperatures averages out any smaller year-to-year fluctuations. For example, during the cool Atlantic, inactive hurricane multidecadal mode of 1970–94, the North Atlantic warmed considerably during 1988 and 1989. However, this warming was followed by cooling in the early 1990s. The switch to the warm Atlantic, active hurricane multidecadal mode did not begin until 1995. We have selected the 6-yr mean SST empirically after trying averages of between 3 and 10 yr. A 6-yr average had the best relationship with U.S. landfalling hurricane activity.

When observed SSTA* and hindcast NTC are combined, ratios between active and inactive years become even more significant. There is a greater than 2:1 ratio for hurricanes along the entire U.S. coast and a 3:1 ratio for all hurricanes along the East Coast. During the 15 largest observed values of SSTA* and hindcast NTC, 15 intense hurricanes made landfall along the U.S. coast, while only 7 intense hurricanes made landfall during the 15 smallest values or a ratio of 2.14:1. When considering only the East Coast, 10 intense hurricanes made landfall during the 15 most active years compared to only two intense hurricanes during the 15 smallest values, or a ratio of 5:1. Although forecasting whether a hurricane will make landfall in any year is not possible, definite skill in issuing probability forecasts is available. Tables 17, 18, and 19 display the top 15–bottom 15 ratios using hindcast NTC and SSTA* compared with observed values of NTC and SSTA* for the entire United States, the Gulf Coast, and the East Coast for named storms, hurricanes, and intense hurricanes. Note that the best ratios are for intense hurricanes along the East Coast of the United States. Table 20 displays landfalling named storms, hurricanes, and intense hurricanes from 1950 to 2000 ranked by cross-validated hindcast NTC and SSTA* and divided into 17-yr segments. Figure 6 displays landfalling hurricanes and intense hurricanes along the East Coast for the 15 largest values and 15 smallest values of cross-validated hindcast NTC and observed SSTA*. There also appears to be some skill in hindcasting named storms along the Gulf Coast, although there is very little difference between active and inactive years for hurricanes and intense hurricanes along the Gulf Coast.

Based on the above discussion, landfall probability equations were developed for named storms, hurricanes, and intense hurricanes along the entire U.S. coastline, the East Coast, and the Gulf Coast. Equations were cal-

TABLE 20. Landfalling named storms, hurricanes, and intense hurricanes for the entire U.S. coast, the Gulf Coast, and the East Coast divided into 17-yr periods based upon cross-validated hindcast NTC and SSTA*.

	Entire U.S. Coast			Gulf Coast			East Coast		
	Cross-validated hindcast NTC + SSTA*	Landfalls	Top third/ bottom third	Cross-validated hindcast NTC + SSTA*	Landfalls	Top third/ bottom third	Cross-validated hindcast NTC + SSTA*	Landfalls	Top third/ bottom third
Named storms									
Highest 17 years	183	68		183	31		183	37	
Middle 17 years	96	53		96	29		96	24	
Lowest 17 years	24	36	1.89	24	18	1.72	24	18	2.06
Hurricanes									
Highest 17 years	183	38		183	13		183	25	
Middle 17 years	96	30		96	17		96	13	
Lowest 17 years	24	17	2.24	24	9	1.44	24	8	3.13
Intense hurricanes									
Highest 17 years	183	15		183	5		183	10	
Middle 17 years	96	12		96	6		96	6	
Lowest 17 years	24	7	2.14	24	5	1.00	24	2	5.00

culated using both hindcast and observed NTC, and the observed NTC equations gave slightly more accurate probability forecasts based on landfalls from 1950 to 2000, and therefore the equations based on observed NTC will be listed here. Each year was ranked by observed NTC and SSTA*, and probabilities of landfall were calculated for each third and fourth of the data. Figure 7 illustrates this process for a probability forecast for intense hurricanes along the entire U.S. coastline. Based on these probabilities, landfalling equations were developed and are listed below. For the U.S. coast:

Named storm probability

$$= 96.06 + 0.02(\text{NTC} + \text{SSTA*}) \quad (3)$$

Hurricane probability

$$= 72.33 + 0.09(\text{NTC} + \text{SSTA*}) \quad (4)$$

Intense hurricane probability

$$= 28.26 + 0.21(\text{NTC} + \text{SSTA*}). \quad (5)$$

For the Gulf Coast:

Named storm probability

$$= 74.87 + 0.09(\text{NTC} + \text{SSTA*}) \quad (6)$$

Hurricane probability

$$= 44.90 + 0.17(\text{NTC} + \text{SSTA*}) \quad (7)$$

Intense hurricane probability

$$= 25.32 + 0.06(\text{NTC} + \text{SSTA*}). \quad (8)$$

For the East Coast:

Named storm probability

$$= 60.10 + 0.12(\text{NTC} + \text{SSTA*}) \quad (9)$$

Hurricane probability

$$= 40.56 + 0.15(\text{NTC} + \text{SSTA*}) \quad (10)$$

Intense hurricane probability

$$= 13.84 + 0.10(\text{NTC} + \text{SSTA*}). \quad (11)$$

Table 21 shows what landfall probabilities would be for selected values of NTC and SSTA*. These equations will be utilized to issue landfall probabilities with this new early-December statistical forecast.

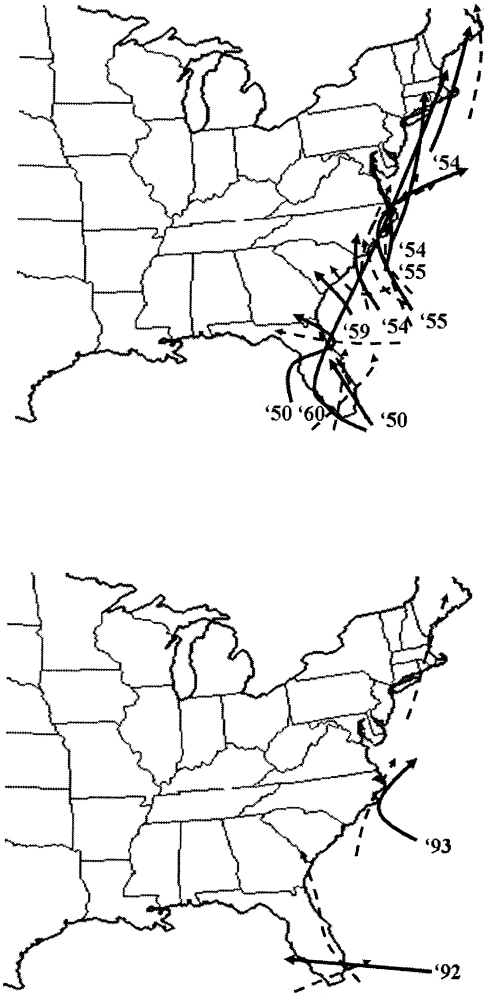

FIG. 6. (top) Landfalling tropical cyclones for the 15 highest cross-validated hindcast NTC + SSTA* values and (bottom) landfalling tropical cyclones for the 15 lowest cross-validated hindcast NTC + SSTA* values, respectively, along the U.S. East Coast. Category 1–2 hurricanes are the dashed lines, and category 3–4–5 hurricanes are the solid lines. Years of landfalling intense hurricanes are as indicated.

8. Future work and conclusions

a. Future work

The early-December statistical forecast hindcast skill over 52 yr of dependent data and the soundness of the physical linkages indicates a strong likelihood that there will be considerable future forecast skill with this scheme. With the currently available NCEP–NCAR reanalysis and the availability of the European Centre for Medium-Range Weather Forecasts (ECMWF) reanalysis in the next few months, the current statistical forecasts utilized to make Atlantic basin hurricane predictions in early April, early June, and early August will also be revised using a similar methodology to that outlined here. The ease of availability of the data and the consistency of the model used to derive the analysis make the reanalysis products a favorable alternative to the time-consuming data acquisition required by the current statistical models for Atlantic hurricane prediction.

As alluded above, the ECMWF is nearing completion of a reanalysis similar to that already done by NCEP–NCAR. Data assimilated into the ECMWF reanalysis model differs somewhat from that assimilated by NCEP–NCAR, and the model used to make the computations is also different. When the ECMWF reanalysis becomes available, we will examine the hindcast skill of our new statistical forecast model to see if there is similar skill using the different reanalysis products. If

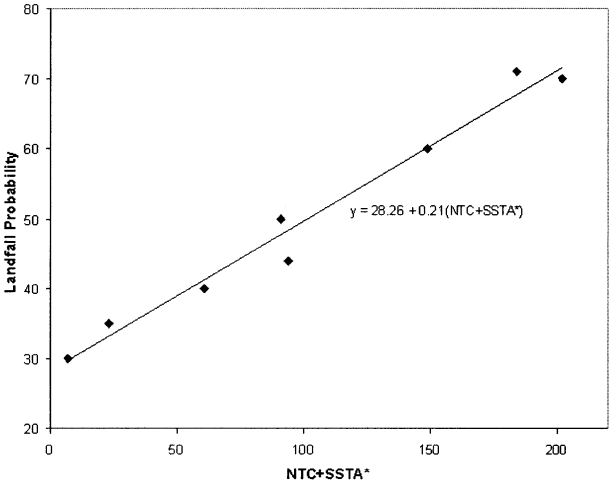

FIG. 7. Landfall probability forecast development for intense hurricanes along the entire U.S. coastline.

TABLE 21. Landfall probabilities for one more or landfalling tropical cyclones for the entire U.S. coast, the Gulf Coast, and the East Coast for NTC + SSTA* values of 0, 50, 100, 150, 200, and 250. Probabilities do not exceed 99% since it is never assured that a particular year will have a landfalling tropical cyclone.

	NTC + SSTA*					
	0	50	100	150	200	250
Entire U.S. coast						
Named storms	96	97	98	99	99	99
Hurricanes	72	77	81	86	90	95
Intense hurricanes	28	39	49	60	70	81
Gulf Coast						
Named storms	75	79	84	88	93	97
Hurricanes	45	53	62	70	79	87
Intense hurricanes	25	28	31	34	37	40
East Coast						
Named storms	60	66	72	78	84	90
Hurricanes	41	48	56	63	71	78
Intense hurricanes	14	19	24	29	34	39

similar skill is shown, it would provide more confidence that the physical relationships discussed here and the concept of this type of extended-range prediction from hindcast analyses are indeed valid.

The development of the reanalysis datasets has provided a valuable tool for individuals interested in forecasting. An accurate forecast of ENSO that improves upon a climatology and persistence forecast is currently unavailable (Landsea and Knaff 2000), and through composite and correlation research, a somewhat more skillful forecast for ENSO is likely possible.

b. Conclusions

The statistical methodology outlined above demonstrates that considerable skill in forecasting Atlantic basin tropical cyclones nearing 50% of the jackknifed hindcast variance for net tropical cyclone (NTC) activity can be achieved by early December of the previous year. It is surprising that the atmosphere would have such a long memory for the frequency of mesoscale weather systems 6–11 months in advance.

Early December forecasts of Atlantic basin tropical cyclone activity will continue to be issued into the foreseeable future, and the statistical methodology outlined in this paper will be utilized as the primary statistical guidance tool. We expect to make further improvements to this statistical forecast technique with continued research.

Acknowledgments. We would like to thank Eric Blake and John Sheaffer for many helpful discussions on tropical cyclone variability. This research was supported by NSF Climate Grant ATM-0087398 and by the research foundation of the Lexington Insurance Group (part of AIG).

APPENDIX

List of Symbols and Acronyms

AO: Arctic Oscillation—The leading empirical orthogonal function (EOF) of sea level pressure poleward of 20°N based on all months from January 1958 to April 1997.
ENSO: El Niño–Southern Oscillation.
EOF: Empirical orthogonal function.
H: Hurricane—A tropical cyclone with sustained low level winds of 74 mph (33 m s^{-1} or 64 kt) or greater.
HD: Hurricane day—A measure of hurricane activity, one unit of which occurs as four 6-h periods during which a tropical cyclone is observed or estimated to have hurricane intensity winds.
IH: Intense hurricane—A hurricane that reaches a sustained 1-min-average 10-m-height wind of at least 111 mph (96 kt or 50 m s^{-1}) at some point in its lifetime. This constitutes a category 3 or higher on the Saffir–Simpson scale (also termed a ''major'' hurricane).
IHD: Intense hurricane day—Four 6-h periods during which a hurricane has intensity of Saffir–Simpson category 3 or higher.
MJO: Madden–Julian oscillation.
NAO: North Atlantic Oscillation—A normalized measure of the surface pressure difference between Iceland and Portugal.
NCAR: National Center for Atmospheric Research, Boulder, Colorado.
NCEP: National Centers for Environmental Prediction, Washington, D.C.
NS: Named storm—A hurricane or tropical storm.
NSD: Named storm day—As in HD but for four 6-h periods during which a tropical cyclone is observed

(or is estimated) to have attained tropical-storm-intensity winds.

NTC: Net tropical cyclone activity—Average seasonal percentage mean of named storms, named storm days, hurricanes, hurricane days, intense hurricanes, and intense hurricane days. Gives overall indication of Atlantic basin seasonal hurricane activity.

PNA: Pacific–North American pattern—One of the most prominent modes in low-frequency variability in the extratropics of the Northern Hemisphere, appearing in all months except June and July.

QBO: Quasi-biennial oscillation—A stratospheric (16–35-km altitude) oscillation of equatorial east–west winds that vary with a period of about 26–30 months or roughly 2 yr, typically blowing for 12–16 months from the east, then reversing and blowing 12–16 months from the west, then back to east again.

SST: Sea surface temperature.

SSTA*: Sea surface temperature anomaly in the North Atlantic Ocean (50°–60°N, 10°–50°W).

TC: Tropical cyclone—A large-scale circular flow occurring within the Tropics and subtropics that has its strongest winds at low levels, including hurricanes, tropical storms, and other weaker rotating vortices.

TOH: Tropical-only hurricanes.

TONS: Tropical-only named storms.

TS: Tropical storm—A tropical cyclone with maximum sustained winds between 39 mph (18 m s^{-1} or 34 kt) and 73 mph (32 m s^{-1} or 63 kt).

REFERENCES

Blake, E. S., 2002: Prediction of August Atlantic basin hurricane activity. Dept. of Atmospheric Science Paper 719, Colorado State University, Fort Collins, CO, 80 pp.

Bove, M. C., J. B. Elsner, C. W. Landsea, X. Niu, and J. J. O'Brien, 1998: Effect of El Niño on U.S. landfalling hurricanes, revisited. *Bull. Amer. Meteor. Soc.,* **79,** 2477–2482.

Elsner, J. B., and C. P. Schmertmann, 1993: Improving extended-range seasonal prediction of intense Atlantic hurricane activity. *Wea. Forecasting,* **8,** 345–351.

——, and ——, 1994: Assessing forecast skill through cross validation. *Wea. Forecasting,* **9,** 619–624.

——, G. S. Lehmiller, and T. B. Kimberlain, 1996: Objective classification of Atlantic hurricanes. *J. Climate,* **9,** 2880–2889.

——, K. B. Liu, and B. Kocher, 2000: Spatial variations in U.S. hurricane activity: Statistics and a physical mechanism. *J. Climate,* **13,** 2293–2305.

Goldenberg, S. B., and L. J. Shapiro, 1996: Physical mechanisms for the association of El Niño and West African rainfall with Atlantic major hurricane activity. *J. Climate,* **9,** 1169–1187.

——, C. W. Landsea, A. M. Mestas-Nuñez, and W. M. Gray, 2001: The recent increase in Atlantic hurricane activity: Causes and implications. *Science,* **293,** 474–479.

Gray, W. M., 1984a: Atlantic seasonal hurricane frequency. Part I: El Niño and 30 mb quasi-biennial oscillation influences. *Mon. Wea. Rev.,* **112,** 1649–1668.

——, 1984b: Atlantic seasonal hurricane frequency. Part II: Forecasting its variability. *Mon. Wea. Rev.,* **112,** 1669–1683.

——, and J. D. Sheaffer, 1991: El Niño and QBO influences on tropical cyclone activity. *Teleconnections Linking Worldwide Climate Anomalies,* M. H. Glantz, R. W. Katz, and N. Nicholls, Eds., Cambridge University Press, 535 pp.

——, C. W. Landsea, P. W. Mielke Jr., and K. J. Berry, 1992a: Predicting Atlantic seasonal hurricane activity 6–11 months in advance. *Wea. Forecasting,* **7,** 440–455.

——, J. D. Sheaffer, and J. A. Knaff, 1992b: Influence of the stratospheric QBO on ENSO variability. *J. Meteor. Soc. Japan,* **70,** 975–995.

——, C. W. Landsea, P. W. Mielke Jr., and K. J. Berry, 1993: Predicting Atlantic basin seasonal tropical cyclone activity by 1 August. *Wea. Forecasting,* **8,** 73–86.

——, ——, ——, and ——, 1994: Predicting Atlantic basin seasonal tropical cyclone activity by 1 June. *Wea. Forecasting,* **9,** 103–115.

——, ——, ——, and ——, 2000: Extended range forecast of Atlantic seasonal hurricane activity and US landfall strike probability for 2001. Dept. of Atmospheric Science Report, Colorado State University, Fort Collins, CO, 22 pp.

Hess, J. C., J. B. Elsner, and N. E. LaSeur, 1995: Improving seasonal hurricane prediction for the Atlantic basin. *Wea. Forecasting,* **10,** 425–432.

Horel, J. D., and J. M. Wallace, 1981: Planetary-scale atmospheric phenomena associated with the Southern Oscillation. *Mon. Wea. Rev.,* **109,** 813–829.

Hoskins, B. J., and D. J. Karoly, 1981: The steady linear response of a spherical atmosphere to thermal and orographic forcing. *J. Atmos. Sci.,* **38,** 1179–1196.

Kalnay, E., and Coauthors, 1996: The NCEP/NCAR 40-Year Reanalysis Project. *Bull. Amer. Meteor. Soc.,* **77,** 437–471.

Klotzbach, P. J., and W. M. Gray, 2003: Forecasting September Atlantic basin tropical cyclone activity. *Wea. Forecasting,* **18,** 1109–1128.

Knaff, J. A., 1993: Evidence of a stratospheric QBO modulation of tropical convection. Department of Atmospheric Science Paper 520, Colorado State University, Fort Collins, CO, 91 pp.

Landsea, C. W., 1993: A climatology of intense (or major) Atlantic hurricanes. *Mon. Wea. Rev.,* **121,** 1703–1713.

——, and W. M. Gray, 1992: The strong association between western Sahel monsoon rainfall and intense Atlantic hurricanes. *J. Climate,* **5,** 435–453.

——, and J. A. Knaff, 2000: How much skill was there in forecasting the very strong 1997–98 El Niño? *Bull. Amer. Meteor. Soc.,* **81,** 2107–2119.

Larkin, N. K., and D. E. Harrison, 2002: ENSO warm (El Niño) and cold (La Niña) event life cycles: Ocean surface anomaly patterns, their symmetries, asymmetries, and implications. *J. Climate,* **15,** 1118–1140.

Lehmiller, G. S., T. B. Kimberlain, and J. B. Elsner, 1997: Seasonal prediction models for North Atlantic basin hurricane location. *Mon. Wea. Rev.,* **125,** 1780–1791.

Neumann, C. J., M. B. Lawrence, and E. L. Caso, 1977: Monte Carlo significance testing as applied to statistical tropical cyclone prediction models. *J. Appl. Meteor.,* **16,** 1165–1174.

Renwick, J. A., and J. M. Wallace, 1996: Relationships between North Pacific wintertime blocking, El Niño, and the PNA pattern. *Mon. Wea. Rev.,* **124,** 1981–1991.

Shapiro, L. J., 1989: The relationship of the quasi-biennial oscillation to Atlantic tropical storm activity. *Mon. Wea. Rev.,* **117,** 1545–1552.

Thompson, D. W. J., and J. M. Wallace, 1998: The Arctic Oscillation signature in the wintertime geopotential height and temperature fields. *Geophys. Res. Lett.,* **25,** 1297–1300.

van Loon, H., and J. C. Rogers, 1978: The seesaw in winter temperatures between Greenland and northern Europe. Part I: General description. *Mon. Wea. Rev.,* **106,** 296–310.

Wallace, J. M., and D. S. Gutzler, 1981: Teleconnections in the geopotential height field during the Northern Hemisphere winter. *Mon. Wea. Rev.,* **109,** 784–812.

Wilks, D. S., 1995: *Statistical Methods in the Atmospheric Sciences: An Introduction.* Academic Press, 464 pp.